*J. Fluid Mech.* (1987), *vol.* 179, *pp.* 345–370
*Printed in Great Britain*



# Nonlinear binary-mode interactions in a developing mixing layer

By D. E. NIKITOPOULOS AND J. T. C. LIU
The Division of Engineering, Brown University, Providence, RI 02912, USA

(Received 4 April 1986 and in revised form 28 October 1986)

In this paper we present the formulation and results of two-wave interactions in a spatially developing shear layer, directed at understanding and interpreting the physical mechanisms that underlie the results of quantitative observation. Our study confirms the existence of Kelly's mechanism that augments the growth of a subharmonic disturbance by extracting energy from its fundamental or vice versa. This mechanism is shown to be strongest in the region where the fundamental begins to return energy to the mean flow and the two wave modes are of comparable energy levels. It is found that the initial conditions and especially the initial phase angle between the two disturbances play a very significant role in the modal development and that of the shear layer itself. A doubling of the shear-layer thickness is shown to take place; the two successive plateaux in its growth are attributed to the peaking in the energy production rates of the fundamental and subharmonic fluctuations.

## 1. Introduction

Sato (1959) appears to have been the first to observe what was then a rather curious development of a subharmonic disturbance in the transition region of a separated plane shear layer. More was subsequently learned from the experiments of Wille (1963), Freymuth (1966), Browand (1966), Miksad (1972, 1973), Winant & Browand (1974) and more recently Ho & Huang (1982), Zhang, Ho & Monkewitz (1985) and Gaster, Kit & Wygnanski (1985). A theoretical explanation of conditions favourable to the subharmonic development in free shear layers was given by Kelly (1967). These conditions include a finite threshold for the fundamental disturbance and more importantly, Kelly's (1967) work implies that a 'favourable' phase relation must exist between the fundamental and its subharmonic. Although Kelly's mechanism was arrived via weakly nonlinear arguments that necessarily involve small amplification rates, the basic physical consequences, rather than the details, have much more universality than the original framework (Liu 1981). On the other hand, for real developing shear layers the disturbance growth rates are anything but small in the incipient transition region as experiments indicate (see, for instance, Ho & Huang 1982).

Quantitative measurements of the disturbance amplitudes indicate that the subharmonic, at half the frequency of the fundamental, peaks further downstream than the fundamental in a spatially developing shear layer (Ho & Huang 1982). Each individual component, in fact, undergoes a life cycle of amplification and decay. Although the peaks in amplitude do not overlap, there is a significant spatial, finite-amplitude region of overlap between the fundamental mode and its subharmonic. The switching in modal content of the disturbances is revealed by the quantitative amplitude measurements (Ho & Huang 1982) to be a gradual process rather than an abrupt one as might have been suggested by visual observations of

dye streaks alone. Of course, we were already cautioned by the work of Williams & Hama (1980). They showed that a linear superposition of constant-amplitude fundamental and subharmonic wave functions in a shear layer could produce interference effects that lead to dye streak accumulation suggesting the switch in modal content, when in fact, each of the wave components is quite distinct.

In this paper we shall present the formulation and results for mode interactions in a spatially developing shear layer, directed at understanding and interpreting the physical mechanisms that underlie the results of quantitative observations. The present work falls into a class of problems involving frequency–mode interactions among two-dimensional spatial structures (or axisymmetric structures in a round jet, Mankbadi 1985). For a discussion of more general situations involving three-dimensional (or helical) structures, see Liu (1987). The basic framework considered is an explicit account of the energy budget of each individual disturbance component as well as that of the mean flow according to Nikitopoulos (1982), Liu & Nikitopoulos (1982) and following their example, Mankbadi (1985) for the case of a jet. This necessitates calculating the rate of energy exchange between the various scales of motion. While the rate of energy exchange between each disturbance mode and the mean flow is fairly well understood (the 'production' mechanism), the rate of energy exchange between modes is still relatively novel. Stuart (1962), although directed at first towards the understanding of the interaction between the fundamental and its harmonic but also appropriate for the subharmonic problem, split the flow quantity for an ensemble of disturbances into odd and even modes. The rate of energy transfer from the even to the odd modes is then $\overline{u_i' u_j' \partial u_i''/\partial x_j}$, where $(\,)'$ denotes odd and $(\,)''$ denotes even modes and the average is taken over the largest periodicity of the disturbances. This is interpreted as the work done by the stresses of the odd modes against the rates of strain of the even modes. The mechanism that we attribute to Kelly (1967) is clear from the present energy transfer consideration in that the phase relation between the stresses of the odd modes and the appropriate rates of strain of the even modes determines the direction of energy transfer and that the mode amplitudes determine the strength of this transfer. However, for a real laboratory shear layer, the fundamental component is one which has the largest initial amplification rate resulting in rather strong interactions with the mean motion. The subharmonic component evolves into a similar situation in a spatial region for which its local amplification rate also reaches a 'momentary' maximum. These interactions with the mean flow scale with an amplitude to the second power via the Reynolds stresses, whereas the mode interactions would scale as a typical amplitude to the third power from the above discussion of the rate of energy transfer. Thus, in a developing shear layer, the individual modal production rate from the mean flow is anticipated to be the dominant mechanism for initial disturbance evolution. In this case, the dominant initial mode interactions would be the implicit nonlinear interactions via the mean flow rather than by the more explicit direct energy transfer between the modes. The latter mechanism is, however, most important in affecting the details of the spatial distribution of the amplitudes and becomes relatively important in the vicinity where the 'production' mechanism from the mean flow changes sign.

## 2. Conservation equations

In laboratory observations of the transition region in shear layers there usually exists modes other than the fundamental and the subharmonic including perhaps initially weak fine-grained turbulence. The latter, coexisting with monochromatic

coherent disturbances, has been the subject of discussion elsewhere (see, for instance, Liu 1981) and will be excluded from consideration here. We shall concentrate on the understanding of coherent mode interactions in an otherwise laminar viscous shear flow. We shall start from the Navier–Stokes equations for an incompressible fluid and split the total flow quantity into that for the mean motion $Q$ and the overall disturbance $\tilde{q}$ consisting of $(q'+q'')$, where $q'$ denotes the odd mode and $q''$ denotes the even mode (Stuart 1962). The mean-flow momentum and continuity equations are obtained following this Reynolds' splitting and averaging,

$$\frac{\overline{\mathrm{D}}U_i}{\mathrm{D}t} = -\frac{\partial \overline{\tilde{u}_i \tilde{u}_j}}{\partial x_j} - \frac{\partial P}{\partial x_i} - \frac{1}{Re}\frac{\partial^2 U_i}{\partial x_i \partial x_j}, \tag{2.1}$$

$$\frac{\partial U_i}{\partial x_i} = 0, \tag{2.2}$$

where appropriate (constant) length and velocity scales are used to make the equations dimensionless, $U_i$ and $P$ are the mean-flow velocity and pressure† respectively, $\tilde{u}_i$ the total disturbance velocity, $x_i$ the spatial coordinates, $t$ the time and $Re$ the Reynolds number. The bar over the substantial derivative indicates that the derivative is taken following the mean flow. The corresponding total disturbance momentum and continuity equations are

$$\frac{\overline{\mathrm{D}}\tilde{u}_i}{\mathrm{D}t} + \tilde{u}_j \frac{\partial U_i}{\partial x_j} = -\frac{\partial \tilde{p}}{\partial x_i} + \frac{1}{Re}\frac{\partial^2 \tilde{u}_i}{\partial x_i \partial x_j} - \frac{\partial(\tilde{u}_i \tilde{u}_j - \overline{\tilde{u}_i \tilde{u}_j})}{\partial x_j}, \tag{2.3}$$

$$\frac{\partial \tilde{u}_i}{\partial x_i} = 0, \tag{2.4}$$

where $\tilde{p}$ is the total disturbance pressure. Equations (2.1)–(2.4) are identical in form with the Reynolds system. Following Stuart (1962), the total disturbance is split into the odd and even modes, $\tilde{u}_i = u_i' + u_i''$. The linear terms in (2.3) and (2.4) are correspondingly split and would retain their respective interpretations in the individual conservation equations for the odd and even modes. The nonlinear effect, through $\partial(\tilde{u}_i \tilde{u}_j - \overline{\tilde{u}_i \tilde{u}_j})/\partial x_j$, deserves further comment. The results from the mode splitting give rise to the nonlinear term $\partial(u_j' u_i'' + u_j'' u_i')/\partial x_j$ for the odd-mode momentum equation, with $\overline{u_i' u_j''} = 0$. The even-mode momentum equation would obtain the even contributions from $\partial(u_i' u_j' - \overline{u_i' u_j'})/\partial x_j$ and $\partial(u_i'' u_j'' - \overline{u_i'' u_j''})/\partial x_j$. However, the mean kinetic energy equations for the odd and even modes would be coupled through the mode interaction mechanism $u_i' u_j' \partial u_i''/\partial x_j$ in what follows.

For the purposes of obtaining the 'amplitude' equations at a later stage, we first obtain the energy equations for the various scales of motion as follows:

mean motion

$$\frac{\mathrm{D}}{\mathrm{D}t}(\tfrac{1}{2}U_i^2) = \underbrace{-(\overline{u_i' u_j'} - \overline{u_i'' u_j''})\left(\frac{\partial U_i}{\partial x_j}\right)}_{\text{(production)}} \underbrace{-\frac{1}{Re}\left(\frac{\partial U_i}{\partial x_j}\right)^2}_{\text{dissipation}} + \underbrace{\frac{\partial}{\partial x_j}\left[\frac{1}{Re}\frac{\partial}{\partial x_j}(\tfrac{1}{2}U_i^2) - PU_j - U_i(\overline{u_i' u_j'} + \overline{u_i'' u_j''})\right]}_{\text{'diffusion'}}; \tag{2.5}$$

† The (constant) density is absorbed into the pressure in all the pressure contributions.

odd modes

$$\frac{\overline{\mathrm{D}}}{\mathrm{D}t}(\tfrac{1}{2}\overline{u_i'^2}) = (-\overline{u_i' u_j'})\frac{\partial U_i}{\partial x_j} - \overline{u_i' u_j' \frac{\partial u_i''}{\partial x_j}} - \frac{1}{Re}\overline{\left[\frac{\partial u_i'}{\partial x_j}\right]^2}$$

production (mode interaction) dissipation

$$+\frac{\partial}{\partial x_j}\left[\frac{1}{Re}\frac{\partial}{\partial x_j}(\tfrac{1}{2}\overline{u_i'^2}) - \overline{p' u_j'} - \overline{u_j'' \tfrac{1}{2} u_i'^2}\right]; \quad (2.6)$$

'diffusion'

even modes

$$\frac{\overline{\mathrm{D}}}{\mathrm{D}t}(\tfrac{1}{2}\overline{u_i''^2}) = (-\overline{u_i'' u_j''})\frac{\partial U_i}{\partial x_j} + \overline{u_i' u_j' \frac{\partial u_i''}{\partial x_j}} - \frac{1}{Re}\overline{\left[\frac{\partial u_i''}{\partial x_j}\right]^2}$$

production (mode interaction) dissipation

$$+\frac{\partial}{\partial x_j}\left[\frac{1}{Re}\frac{\partial}{\partial x_j}(\tfrac{1}{2}\overline{u_i''^2}) - \overline{p'' u_j''} - \overline{u_j'' \tfrac{1}{2} u_i''^2} - \overline{u_i'' u_i' u_j'}\right]. \quad (2.7)$$

'diffusion'

The usual Reynolds average has been used and we note that the products $\overline{u_i' u_j''}$ are uncorrelated but that the triple products such as $\overline{u_i' u_j' \partial u_i''/\partial x_j}$ are. These latter products are interpreted as the work done by the stresses of the odd modes against the appropriate rates of strain of the even modes and are responsible for the net energy transfer between the odd and even modes. Both the even and odd modes have their respective production mechanism, responsible for the extraction of energy from or a return of energy to the mean shearing motion. The remaining mechanisms include the rate of viscous dissipation of the various scales of motion and of 'diffusion' by viscosity and by the fluctuations.

The discussion is so far general in that we have not specified whether the problem is spatial or temporal. For the spatial problem the Reynolds average is then the time average, the periodicity is in time and the amplitudes (or 'envelopes') of the fluctuations grow and decay spatially. In the temporal problem, the Reynolds average is spatial, connected with the spatial periodicity and the amplitude of fluctuations evolves in time. In the following we shall study the observed or observable spatially developing shear layer for which the fluctuations have periodicity in time. In this case the odd modes consist of frequencies $\beta, 3\beta, \ldots, (2n-1)\beta$ and the even modes consist of $2\beta, 4\beta, \ldots, 2n\beta$, where $n$ is an integer. Thus mode $u_i''(2\beta)$ would correspond to, say, the fundamental component and $u_i'(\beta)$ would then be its subharmonic. In §3 we shall consider the nonlinear interaction between modes $2\beta$ and $\beta$ in a developing shear layer, the simplest case of mode interactions.

## 3. Two-mode interactions

In this section we shall apply the general framework obtained previously to study the two-mode interaction problem. The even mode $u''$ would thus be interpreted as that of the fundamental mode with frequency $2\beta$; the odd mode $u'$ would be its subharmonic of frequency $\beta$. With the objective of obtaining the 'amplitude' or 'envelope' equations, in terms of the observable kinetic-energy content across the shear layer for each mode, we begin with (2.5)–(2.7) for a thin shear layer for which the boundary-layer type of approximations hold for the mean quantities. The

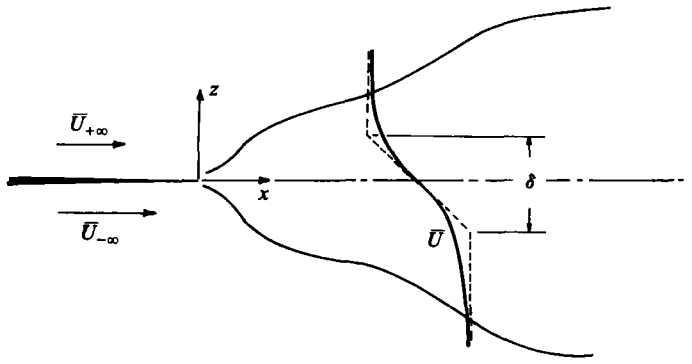


FIGURE 1. The mixing-layer schematic.

schematical representation of the shear layer is shown in figure 1. The simplified kinetic-energy equations are then integrated across the plane shear layer to give

$$\frac{1}{2}\frac{\mathrm{d}}{\mathrm{d}x}\left[\int_{-\infty}^{0} U(U^2-U_{-\infty}^2)\,\mathrm{d}z+\int_{0}^{\infty} U(U^2-U_{+\infty}^2)\,\mathrm{d}z\right]=-\int_{-\infty}^{\infty}(-\overline{u'w'}-\overline{u''w''})\frac{\partial U}{\partial z}-\overline{\Phi}, \tag{3.1}$$

$$\frac{1}{2}\frac{\mathrm{d}}{\mathrm{d}x}\int_{-\infty}^{\infty} U(\overline{u'^2+w'^2})\,\mathrm{d}z=\int_{-\infty}^{\infty}(-\overline{u'w'})\frac{\partial U}{\partial z}\mathrm{d}z+\int_{-\infty}^{\infty}\left[\overline{u'^2\frac{\partial u''}{\partial x}}+\overline{u'w'\left(\frac{\partial u''}{\partial z}+\frac{\partial w''}{\partial x}\right)}+\overline{w'^2\frac{\partial w''}{\partial z}}\right]\mathrm{d}z-\overline{\phi'}, \tag{3.2}$$

$$\frac{1}{2}\frac{\mathrm{d}}{\mathrm{d}x}\int_{-\infty}^{\infty} U(\overline{u''^2+w''^2})\,\mathrm{d}z=\int_{-\infty}^{\infty}(-\overline{u''w''})\frac{\partial U}{\partial z}\mathrm{d}z+\int_{-\infty}^{\infty}\left[\overline{u'^2\frac{\partial u''}{\partial x}}+\overline{u'w'\left(\frac{\partial u''}{\partial z}+\frac{\partial w''}{\partial x}\right)}+\overline{w'^2\frac{\partial w''}{\partial z}}\right]\mathrm{d}z-\overline{\phi''}, \tag{3.3}$$

where $x$ is the streamwise coordinate measured from the start of the mixing layer, $z$ is the vertical coordinate measured from the centre of the mixing layer; $u, w$ are the $x, z$ fluctuation velocities; $U$ is the mean velocity with $\pm\infty$ denoting the upper (say, slower) and lower free streams, respectively; $\overline{\Phi}$ is the integral of mean-flow viscous dissipation and $\overline{\phi'}$ and $\overline{\phi''}$ represent the corresponding dissipation rates of the fluctuations. Equations (3.1)–(3.3), where two-dimensional wavy disturbances in a two-dimensional mean flow have been assumed, form the basis for obtaining the evolution equations for the measurable energy content of the disturbances across the shear layer.

### 3.1. *Shape assumptions*

Following earlier work (see, for instance, Stuart 1958; Ru-Sue Ko, Kubota & Lees 1970; Liu & Lees 1970; Liu 1981; Alper & Liu 1978), the 'closures' for the disturbances are obtained by assuming the separable form of the product of an unknown finite amplitude $A_n(x)$ with a vertical distribution function given by the local linear stability theory,

$$\begin{pmatrix}u'\\w'\end{pmatrix}=\left[A_1(x)\begin{pmatrix}\phi_1'\,\mathrm{e}^{-\mathrm{i}\beta t}\\-\mathrm{i}\alpha_1\phi_1\,\mathrm{e}^{-\mathrm{i}\beta t}\end{pmatrix}+\begin{pmatrix}\text{c.c.}\\\text{c.c.}\end{pmatrix}\right]\quad\text{(subharmonic)},$$

$$\begin{pmatrix}u''\\w''\end{pmatrix}=\left[A_2(x)\begin{pmatrix}\phi_2'\,\mathrm{e}^{-2\mathrm{i}\beta t-\mathrm{i}\theta}\\-\mathrm{i}\alpha_2\phi_2\,\mathrm{e}^{-2\mathrm{i}\beta t-\mathrm{i}\theta}\end{pmatrix}+\begin{pmatrix}\text{c.c.}\\\text{c.c.}\end{pmatrix}\right]\quad\text{(fundamental)},$$

where $\phi_i$ here denotes the eigenfunction of the local linear theory and is a function of the rescaled vertical variable $\eta = z/\delta(x)$; $\delta(x)$ is a lengthscale of the mean flow yet to be identified and $(\,)'$ denotes differentiation with respect to $\eta$; $\beta = 2\pi f\delta(x)/\overline{U}$ is the dimensionless local (Strouhal) frequency, $f$ is the physical frequency and $\overline{U} = \frac{1}{2}(U_\infty + U_{-\infty})$. The local wavenumbers $\alpha$ are also scaled by $\delta(x)$. The angle $\theta$ is the relative phase between the fundamental component ($2\beta$) and its subharmonic ($\beta$) and c.c. denotes the complex conjugate. The velocities and lengths are considered to be made dimensionless by $\overline{U}$ and $\delta_0$ (so that $\delta(0) = 1$), and time by $\delta_0/\overline{U}$. These two-dimensional disturbances have their vorticity axis perpendicular to the direction of the free streams.

For the mean flow we shall assume a hyperbolic tangent-type profile, which has experimentally proven to be very close to reality away from the splitter plate into the developed mixing-layer region (Wygnanski *et al.* 1979; Fiedler *et al.* 1981; Ho & Huang 1982),

$$U = 1 - R\tanh\eta,$$

where

$$R = \frac{U_{-\infty} - U_{+\infty}}{U_{-\infty} + U_{+\infty}}$$

is the velocity ratio of the shear layer. Since $\eta = z/\delta(x)$, it is now understood that $\delta(x)$ is the half-maximum slope thickness of the shear layer. This characterizes the mean motion and must be jointly determined with the amplitudes $A_i(x)$ of the finite disturbances.

Both shape functions $\phi_1$ and $\phi_2$ are taken to be governed locally by the Rayleigh equation (see Liu & Merkine 1976) according to linear stability analysis with the appropriate boundary conditions

$$(U-c)(\phi'' - \alpha^2\phi) - \phi U'' = 0,$$

where $c$ is the phase velocity scaled by the mean velocity $\overline{U}$ of the two free streams. This, of course, is an approximation since the viscous terms have been dropped. We deal here with an inflexional mean-velocity profile which is dynamically unstable and thus the inviscid equation suffices. The Rayleigh equation yields solutions that correspond to amplified disturbances up to the point $\beta = 1$ of neutral stability. In the neighbourhood of this point and for values of $\beta$ larger than 1 (corresponding to damped disturbances) the equation becomes singular. In order to obtain solutions in the locally damped region use is made of a complex integration contour scheme first discussed by Lin (1955) and successfully applied by Mack (1965) and Zaat (1958) for the case of a boundary layer. The amplification rates $-\alpha_i$ versus $\beta$ are shown in figure 2, providing the necessary 'state' diagram for initial disturbances in the subsequent nonlinear problem.

The eigenfunctions $\phi_1$ and $\phi_2$ are normalized so as to render $|A_1(x)|^2$ and $|A_2(x)|^2$ to corresponding energy densities of each mode of the finite disturbances such that the mode energy contents across the shear layer are

$$E_1(x) = \frac{1}{2}\int_{-\infty}^{+\infty} (\overline{u'^2 + w'^2})\,\mathrm{d}y = |A_1(x)|^2\,\delta(x),$$

$$E_2(x) = \frac{1}{2}\int_{-\infty}^{+\infty} (\overline{u''^2 + w''^2})\,\mathrm{d}y = |A_2(x)|^2\,\delta(x).$$

This is similar to Ho & Huang's (1982) $E(f)$, except that their energy content refers to the contribution by $u$ alone. The normalization of the local eigenfunctions allows us to relate the energy content to the amplitude.

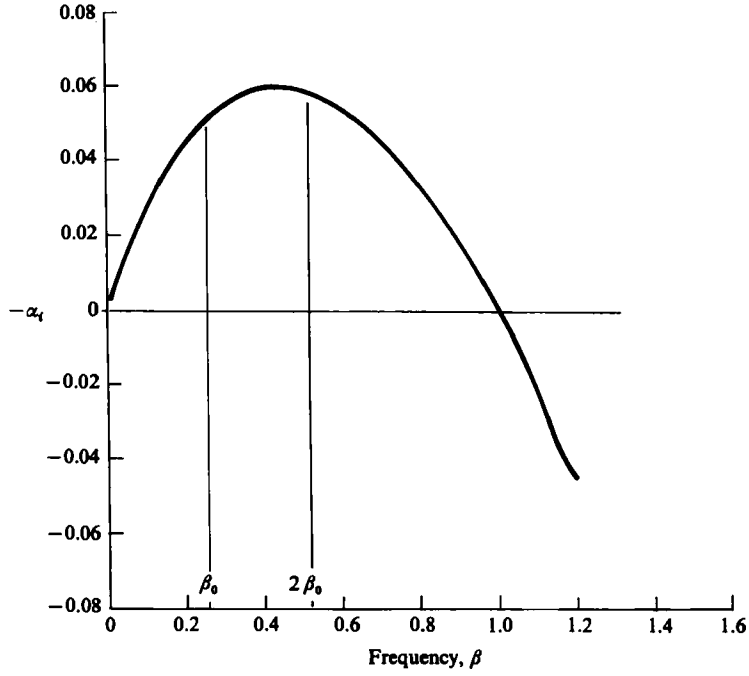


FIGURE 2. Amplification rates $-\alpha_i$ versus frequency parameter $\beta$.

### 3.2. *The nonlinear interaction problem*

After substituting the shape assumptions into (3.1)–(3.3) we obtain three first-order nonlinear differential equations describing the streamwise evolution of $\delta, E_1$ and $E_2$ (or $\delta, |A_1|^2$ and $|A_2|^2$):

mean flow

$$I_m \frac{d\delta}{dx} = \frac{I_{rs2}(\delta) E_2 + I_{rs1}(\delta) E_1}{\delta} + \frac{(1/Re_0) I_d}{\delta}; \tag{3.4}$$

subharmonic

$$\overline{I_1(\delta)} \frac{dE_1}{dx} = \frac{I_{rs1}(\delta) E_1}{\delta} - \frac{I_{21}(\delta) E_1 E_2^{\frac{1}{2}}}{\delta^{\frac{3}{2}}} - \frac{(1/Re) I_{d1}(\delta) E_1}{\delta^2}; \tag{3.5}$$

fundamental

$$\overline{I_2(\delta)} \frac{dE_2}{dx} = \frac{I_{rs2}(\delta) E_2}{\delta} + \frac{I_{21}(\delta) E_1 E_2^{\frac{1}{2}}}{\delta^{\frac{3}{2}}} - \frac{(1/Re_0) I_{d2}(\delta) E_2}{\delta^2}. \tag{3.6}$$

Equations (3.4)–(3.6) are subject to the initial conditions $E_1(0) = E_{10}$, $E_2(0) = E_{20}$ and $\delta(0) = 1$; with $\beta(0) = \beta_0$ chosen to correspond to the physical frequency of the subharmonic, the specified $\overline{U}$ and the initial physical lengthscale of the mean flow $\delta_0$. This lengthscale is identified with the initial half-maximum slope thickness. The advection integrals are $I_m$, $I_1(\delta)$ and $I_2(\delta)$. Integrals involving wave disturbances are dependent on $\delta(x)$ through the dependence of the local instability properties on the local frequency parameter $\beta$, except for $I_1$ and $I_2$ that are very nearly constant and have been replaced in the equations by their average value. The production integrals are $I_{rs1}(\delta)$ and $I_{rs2}(\delta)$ and the mode-energy exchange integral is $I_{21}(\delta)$. The viscous dissipation integrals are $I_d$, $I_{d1}(\delta)$ and $I_{d2}(\delta)$. The Reynolds number is $Re_0 = \overline{U}\delta_0/\nu$.

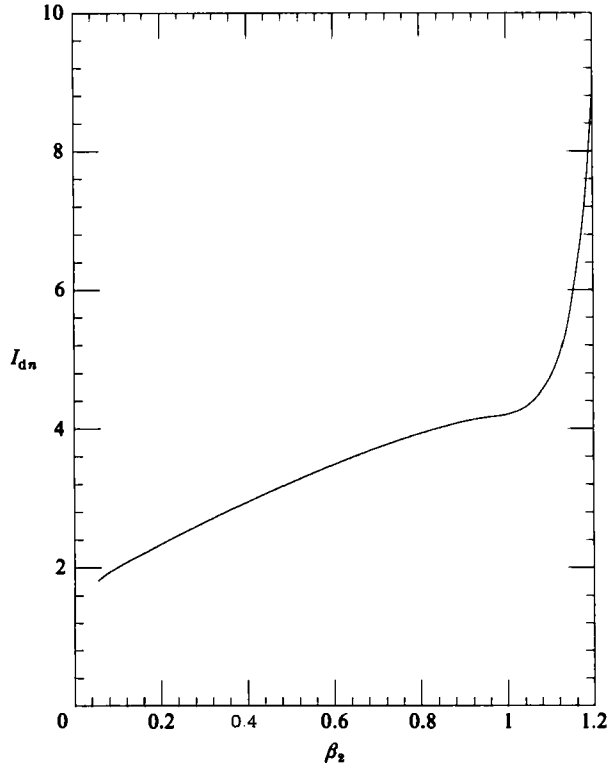


FIGURE 3. Mode-viscous-dissipation integral $I_{dn}$ as function of frequency parameter $\beta$.

The subscripts 1 and 2, as interpreted previously, denote the subharmonic and fundamental, respectively. The detailed definition of these integrals are given in the Appendix. Their physical meaning is identifiable through (3.1)–(3.3). The mean-flow integrals $I_m$ and $I_d$ are constants for a fixed velocity-ratio parameter $R$, whereas integrals involving the wavy disturbances are tabulated functions of the dependent variable $\delta(x)$, again for a fixed $R$. It was sufficient to use the Rayleigh equation in obtaining the characteristics of such integrals (see, for instance, Liu & Merkine 1976); they are thus not explicit functions of the Reynolds number.

### 3.3. *Mode-dependent interaction integrals*

Prior to discussing the numerical applications, it would be most instructive to show the behaviour of the mode-related integrals in (3.4)–(3.6). These are 'universal' functions of the local shear layer thickness $\delta(x)$, or more precisely of the local frequency parameter $\beta = 2\pi f\delta(x)/\overline{U}$ for a fixed frequency $f$. The value of the velocity-ratio parameter $R$ is taken to be 0.31. The mode viscous dissipation integral $I_{dn}$ is shown in figure 3 as function of $\beta$. The mode-advection integral $I_n$ slowly varies between 0.965 and 1 in the same interval of $\beta$ and is thus not shown. The mode-production integral $I_{rsn}$ is shown in figure 4. The integrals $I_{rs1}$ and $I_{rs2}$ are the subharmonic and fundamental 'production' integrals, respectively. Their sign controls the energy flow to or from the mean flow. When they are positive the disturbance wave component is amplified by extracting energy from the mean flow and when negative the disturbance is 'damped' by returning energy to the mean motion. The latter phenomenon is rather similar to hydrodynamic stability interpretations and is now

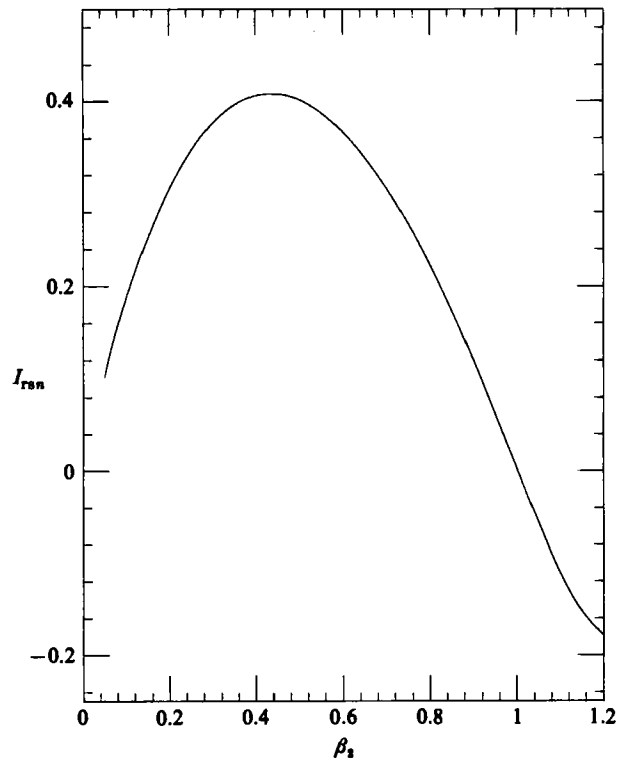


FIGURE 4. Mode-production integral $I_{rsn}$ as function of frequency parameter $\beta$.

widely observed in developing free shear flows. The interpretation of $n = 1$ and 2 is that the frequency ratio $\beta_1 : \beta_2$ be maintained as 1:2. That is, if the physical frequency of the fundamental ($\beta_2$) has the value $f_2 = 2f$ then the subharmonic component ($\beta_1$) has the value $f_1 = f$, both at the same $\delta(x)$. Thus, in figure 4, if the fundamental mode is initiated at $\beta_2 = 0.4426$ where $I_{rs2}$ is maximum, the subharmonic would be at $\beta_1 = 0.2213$ where $I_{rs1}$ is smaller and to the left of the hump of the production-integral curve. In this case, as $\delta(x)$ increases the respective production integrals then traverse along this curve with $I_{rs2}$ becoming negative first while $I_{rs1}$ passes through its maximum value.

The binary-mode-interaction integral $I_{21}$ is shown in figure 5, with the relative phase angle $\theta$ as a parameter. We have chosen to interpret $I_{21}$ as a function of $\beta_1$ in figure 5 (while keeping track of $\beta_2$, for the same $\delta(x)$). The integral $I_{21}$, which represents the interaction between the fundamental and the subharmonic, controls the energy flow between the two modes via its magnitude and sign. The subharmonic draws energy from the fundamental when $I_{21} < 0$ and loses energy to the fundamental when $I_{21} > 0$. In turn the sign of this integral is controlled by the phase angle between the two modes $\theta$ and is of great significance to the role of the binary-mode-interaction mechanism. In effect $\theta$ is the governing parameter that dictates whether the subharmonic grows at higher (Kelly 1967) or lower amplification rates than those dictated by linear stability analysis.

The present formulation is intended to solve the streamwise development problem from the use of the local linear theory in the evaluation of the interaction integrals. It is, however, crucial to reconcile any similarities with the pioneering work of Kelly

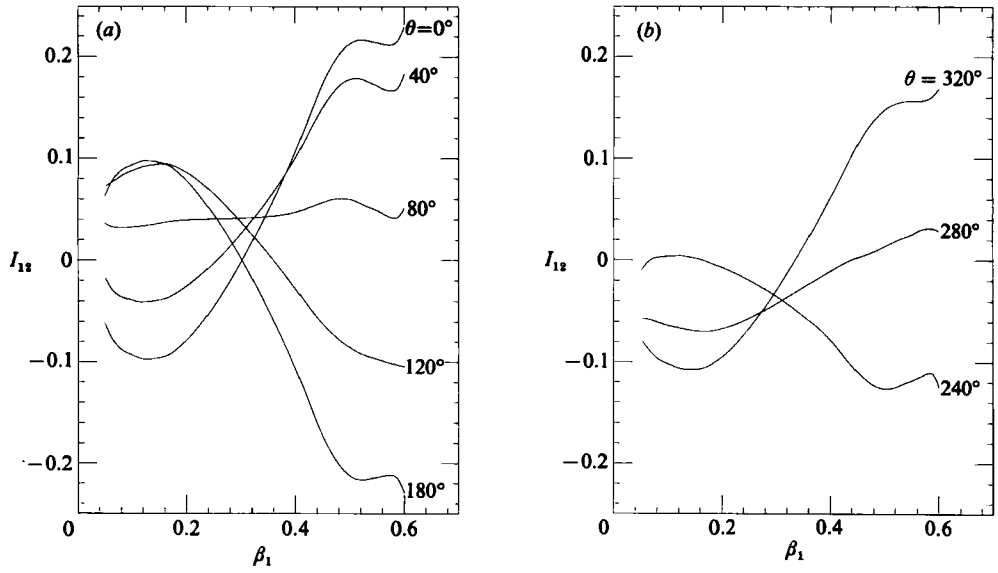


FIGURE 5(*a*, *b*). Binary-mode-interaction integral $I_{21}$ as function of frequency parameter $\beta$ with relative phase angle $\theta$ as a parameter.

(1967) for a parallel flow and weak nonlinearities. In the context of the present spatial problem, Kelly's analysis falls in the local region where the fundamental component is most amplified. The most amplified mode occurs at $\beta_2 = 0.4426$ in figure 2 and thus $\beta_1 = 0.2213$, where the subharmonic is amplifying owing to the mean flow. In figure 5, where the horizontal axis is $\beta_1$, a vertical line drawn from $\beta_1 = 0.2213$ cuts across values of the binary-mode-interaction integral for various relative phase angles $\theta$. For this situation, $0° \leqslant \theta < 60°$ give rise to $I_{21} < 0$, implying energy transfer from the fundamental to the subharmonic. Thus the mean-flow amplification of the subharmonic component is augmented by the fundamental within this range of phase angles. The opposite is true as $\theta \to \pi$ as shown in figure 5 for $\beta_1 = 0.2213$. This is consistent with Kelly (1967). We again emphasize that the temporal, parallel-flow problem that Kelly discussed occurs 'momentarily' at one streamwise location corresponding to $\beta_2 = 0.4426$ and $\beta_1 = 0.2213$ in the context of the present *developing*-shear-layer problem. In our problem, the development of the amplitudes is a strong function of the initial and spectral conditions, dictated by the nonlinear interactions according to (3.4)–(3.6). The realistic outcome is not necessarily anticipated from considerations based on parallel flow.

## 4. Results and discussion

The theoretical formulation, presented in the previous sections of this paper, indicates that the initial conditions ($\beta_0, E_{20}, E_{10}$) along with the phase angle $\theta$ are parameters that play a significant role in the development of the two interacting wave modes and, subsequently, the development of the shear layer. The phase angle $\theta$ between the fundamental wave component and its subharmonic has been shown to be the parameter responsible for the direct energy transfer between the two wave modes. The initial dimensionless frequency $\beta_0$ has two significant effects. It defines, on one hand, the initial amplification rate and the downstream amplification 'history'

of each wave from the interaction with the mean flow and, on the other, the nature of the initial interaction between the two waves. The strength of the interaction between the waves as well as that between the waves and the mean flow is also controlled by the initial energy densities $E_{20}$ and $E_{10}$ of the fundamental and subharmonic, respectively, as pointed out by Kelly (1967). Finally, the Reynolds number $Re_0$ influences the intensity of viscous dissipation for all the components of the flow. This parameter is of minor importance in this formulation where the local linear solution is independent of the Reynolds number, and viscous dissipation is weak compared to the other mechanisms present.

We have solved the nonlinear interaction problem, formulated by (3.4)–(3.6), for different values of the controlling parameters, in order to bring forth their effect on the development of the shear layer and the interactions between the three components of the flow. These results are presented first, and would provide a basis for possible further quantitative experiments. We then present results for conditions based on the experiment of Ho & Huang (1982) in order to compare our theoretical results with their measurements.

### 4.1. *Effect of the phase angle* $\theta$

To better illustrate the role of the phase angle $\theta$ on the development of the shear layer and the energy content of the interacting modes, we have chosen to examine two cases. For fixed initial energy densities $E_{20} = 0.68\ 10^{-4}$ and $E_{10} = 0.12\ 10^{-4}$ and fixed Reynolds number $Re_0 = 71$ we have solved the interaction problem for low and high initial frequency parameters. We have carried out the calculations for various representative values of the phase angle. The initial frequency parameter characterizing each case is, by our choice, that of the subharmonic wave.

#### 4.1.1. *Low initial frequency parameter*

The streamwise development of the energy levels of the fundamental ($E_2$) and subharmonic ($E_1$) waves, scaled by the corresponding initial values, are presented in figure 6(*a*) for phase angles of 0° and 180°, as well as for the case where the direct wave-interaction mechanism is artificially neglected. In the latter case, indirect coupling between the waves is through their nonlinear interactions with the mean flow. The initial subharmonic frequency parameter is taken to be $\beta_0 = 0.075$, giving a fundamental frequency of $2\beta_0 = 0.15$. The two modes start at a frequency parameter much smaller than the most amplified case in terms of linear stability theory (figure 2). Thus, it is expected that for this case in order to approximate the flow more accurately one would have to take more wave modes that fall within the unstable range into account (a mode of $3\beta$ for instance). In the present study, however, we are concentrating on the two-wave interactions (namely the one between subharmonic and fundamental) and our discussion will be carried out in this context only, leaving the interactions between three or more modes to future investigation. Naturally the fundamental experiences maximum amplification (among the two modes) first while the subharmonic grows at a lower rate as can be seen from figure 6(*a*).

In the early stage of the development of the two modes when $\theta = 0°$ the subharmonic draws energy from the fundamental component because the two-mode-interaction integral $I_{21}$ is negative. Therefore the subharmonic is growing, in that region, at higher amplification rates than those predicted by linear stability analysis from its interaction with the mean flow only. This is evident from the comparison with the decoupled case in the region $0 < x/\delta_0 < 55$, as presented in

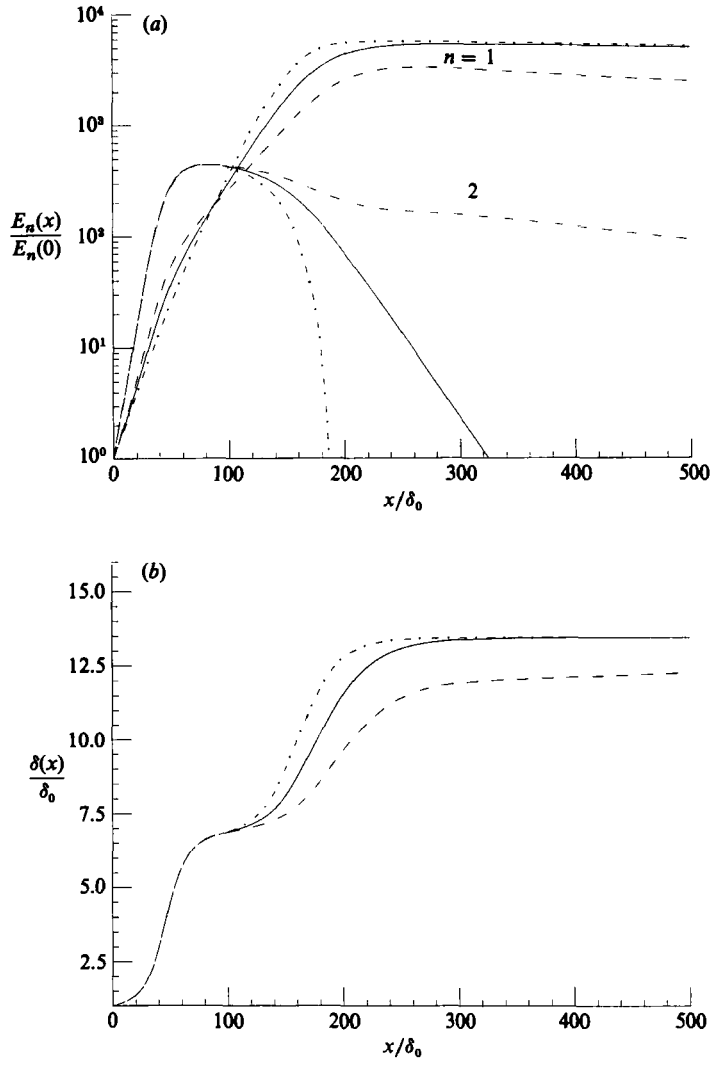


FIGURE 6. Effect of relative phase angle: (*a*) development of modal energy content and (*b*) mean-flow growth for low initial frequency parameter. ($\theta = 0°$ (– – – –), 180° (– · – · –) and decoupled (——) cases; $E_{10} = 0.12 \times 10^{-4}$, $E_{20} = 0.68 \times 10^{-4}$, $\beta_0 = 0.075$, $Re_0 = 71$).

figure 6(*a*). This situation persists until the fundamental goes through maximum amplification (for a local $\beta_2 \leqslant 0.6$ as indicated in the discussion of the two-mode-interaction integral) and is in agreement with the conclusion of Kelly (1967). In the same region, for the case of $\theta = 180°$, the interaction integral $I_{21}$ is positive and the subharmonic loses energy to the fundamental component, thus growing at a lower amplification rate, as shown in figure 6(*a*). The comparison with the decoupled case, in this region, shows that the wave interaction has a greater effect on the development of the subharmonic because its interaction with the mean flow is much weaker than that of the fundamental. The extraction of energy from the mean flow is the dominant energy supply for the fundamental component and is responsible for the peak in $E_2$. In the strongly nonlinear region, for values of the fundamental-frequency parameter $\beta_2$ higher than 0.6 ($x/\delta_0 > 55$ in figure 6*a*) the sign of the

two-mode-interaction term, $I_{21} E_1 E_2^{\frac{1}{2}}/\delta^{\frac{3}{2}}$, in (3.5) and (3.6) is reversed and therefore the subharmonic loses energy to the fundamental component when $\theta = 0°$. Because of this interaction the subharmonic wave grows at a lower rate and the fundamental persists downstream even when it starts losing energy to the mean flow. This mechanism accounts for the lower and later peak of the subharmonic energy $E_1$ compared to the decoupled case.

In the case of $\theta = 180°$, the opposite situation to the $\theta = 0°$ case takes place in the strongly nonlinear region. The subharmonic, drawing energy from the fundamental, grows faster and to a higher peak, while the fundamental is quickly damped by the combined loss of energy to the subharmonic component and mean flow. The wave interaction is the decisive factor for the survival of the fundamental far downstream, since there it is being damped by returning energy to the mean flow, where $I_{rs2} < 0$ (figure 4). The subharmonic is affected by the wave interaction to a relatively small extent. This becomes obvious from the comparison with the decoupled case in figure 6(*a*).

From (3.4), it is obvious that the mean flow will spread as long as energy is lost from the mean flow, whether it is due to viscous dissipation or energy transfer to the fluctuations (Ru-Sue Ko, Kubota & Lees 1970; Liu & Lees 1970; Liu 1987). The resulting growth of the mean flow is shown in figure 6(*b*). The initial rapid growth is governed by the strong interaction of the amplified fundamental disturbance with the mean flow and remains unaffected by the interaction between the two disturbances, which in this region is very weak. The first plateau is due to the peak in the fundamental, the second to the peaking of the subharmonic. These plateaux are associated with the observed phenomenon of negative energy production from the mean (see, for instance, Fiedler *et al.* 1981) that occurs when the sign of the Reynolds stress $-\overline{\tilde{u}\tilde{w}}$ of a particular wave mode of coherent structure is opposite to that of the mean-flow rate of strain $\partial U/\partial z$ and the production integral $I_{rsn} < 0$, thus tending to halt the shear-layer growth. After the first plateau the growth of the mean flow is again rapid because of the amplification of the subharmonic from extraction of energy from the mean flow. However, the interaction of the two modes seems to play some role on this development. In the case of $\theta = 180°$ the growth of the mean is somewhat steeper because of the extra energy that is channelled into the subharmonic wave from the fundamental component. The opposite is true in the case where $\theta = 0°$ and the plateau that results from the saturation of the subharmonic is somewhat lower. The shear-layer thickness due to the subharmonic is very nearly double that due to the fundamental in figure 6(*b*). That is, the ratio of the two plateaux is nearly two. However, this is somewhat dependent upon the initial conditions, as we shall show later, and ought not to be a general rule.

### 4.1.2. *High initial frequency parameter*

The streamwise development of the energy levels of the fundamental ($E_2$) and subharmonic ($E_1$) waves, scaled by the corresponding initial values, are presented in figure 7(*a*) for phase angles of 0°, 80° and 180°, as well as for the decoupled case. The initial energy densities and Reynolds number are the same as in the case of low initial frequency parameter while the value of the latter is now taken to be $\beta_0 = 0.18$ for the subharmonic and $2\beta_0 = 0.36$ for the fundamental component. The latter is slightly less than the initially most amplified Strouhal frequency.

Both disturbances experience a higher initial amplification than in the previous case because their initial frequency parameters are closer to the one corresponding to the most amplified disturbance. A consequence of this is that the two-wave

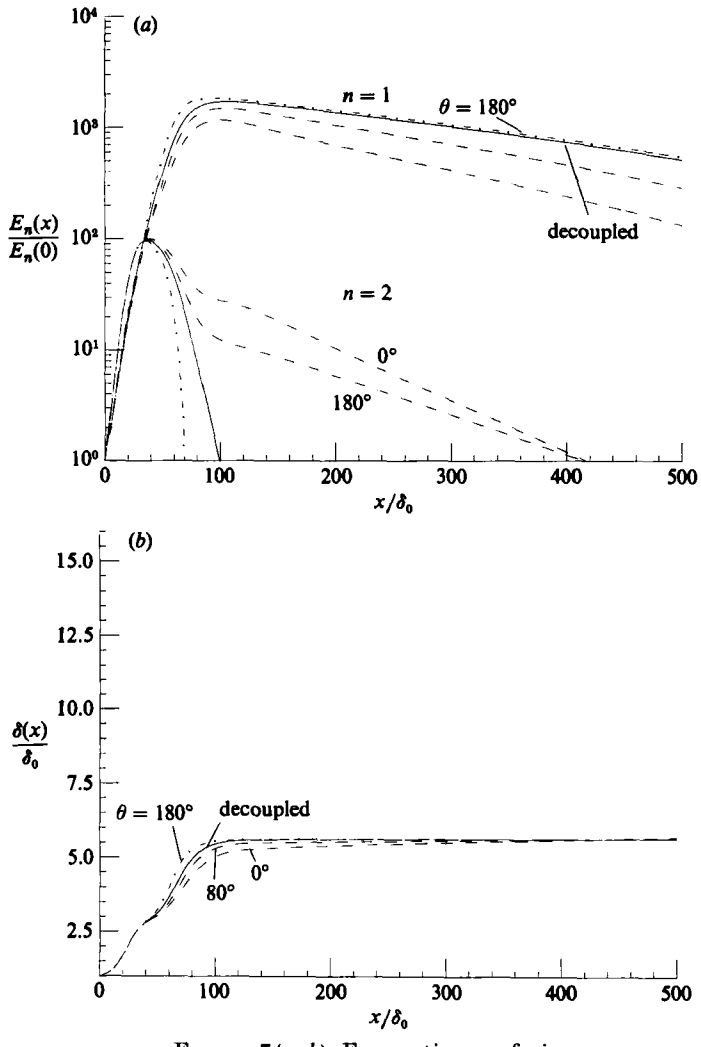


FIGURE 7 (*a*, *b*). For caption see facing page.

interaction mechanism is much weaker than the interaction of both wave components with the mean. Subsequently the initial development of $E_1$ and $E_2$ is essentially unaffected by the modal interaction as shown in figure 7 (*a*). The two-wave interaction becomes important in the strongly nonlinear region, after the fundamental has reached its peak, in the same manner as in the previous case of low initial frequency parameter. The case of $\theta = 80°$ is characterized by a weaker modal interaction than that of $\theta = 0°$, as one can expect from the magnitude of the respective interaction integrals (figure 4). The energy flow is from the subharmonic to the fundamental component for both of these phase angles, in the strongly nonlinear region. The resulting growth of the mean flow, which is shown in figure 7 (*b*), indicates the same general trends observed for the low-initial-frequency-parameter case.

The two-wave interaction mechanism has a dual effect on the modal development. It affects the amplification rate of the subharmonic directly by providing energy from the fundamental and indirectly by increasing the energy gained from the mean, since this gain is proportional to $E_1$. These two effects are of course coupled. The direct

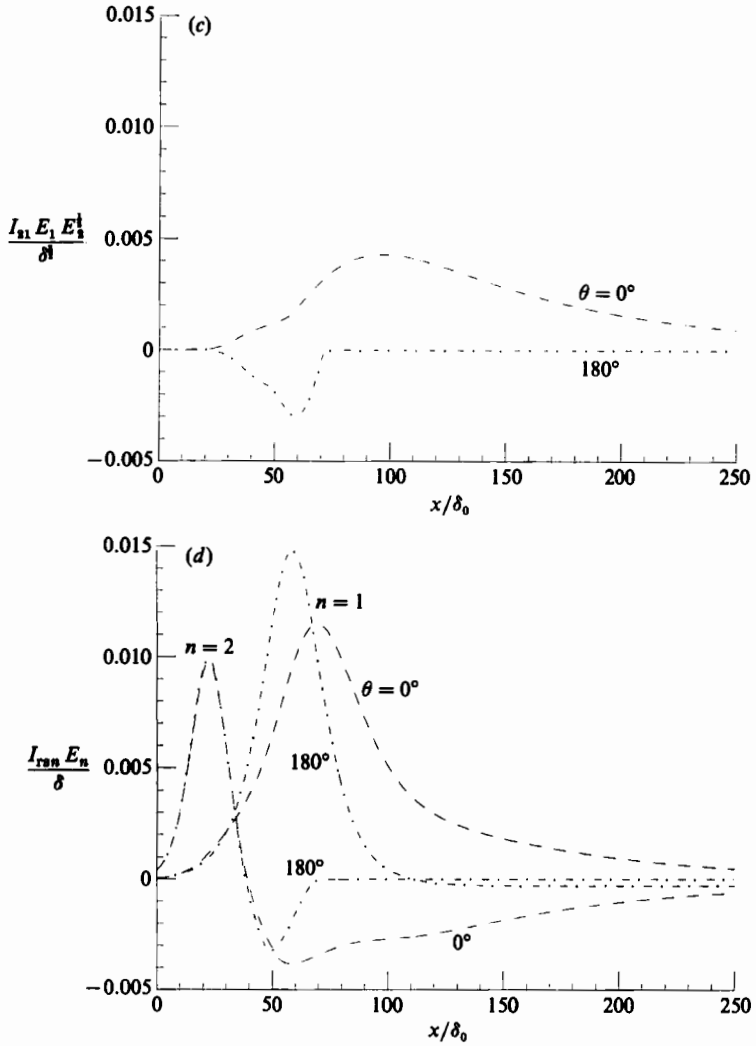


FIGURE 7. Effect of relative phase angle: (*a*) development of modal energy content, (*b*) mean-flow growth, (*c*) mode-production development and (*d*) development of binary-mode interaction for high initial frequency parameter. $E_{10} = 0.12 \times 10^{-4}$, $E_{20} = 0.68 \times 10^{-4}$, $\beta_0 = 0.18$, $Re_0 = 71$).

two-wave interaction mechanism is represented by the term $I_{21}E_1E_{\frac{1}{2}}^{\frac{1}{2}}/\delta^{\frac{3}{2}}$, and is shown in figure 7 (*c*). The indirect wave-interaction effect can be realized by comparing the mean-subharmonic interaction term, $I_{rs1}E_1/\delta$, for the cases of $\theta = 0°$ and $\theta = 180°$ as presented in figure 7 (*d*). It also can be seen from figure 7 (*c*, *d*) that the indirect effect of the two-wave-interaction mechanism is more significant, because the energy exchange with the mean is the controlling factor in the growth of the subharmonic in this particular case.

### 4.2. *Effect of the initial frequency parameter* $\beta_0$

The streamwise development of the energy levels of the two wave modes are shown in figure 8 (*a*) for three different initial frequency parameters and for a phase angle $\theta = 0°$. The initial frequency parameter, as pointed out earlier, sets the initial amplification rate of the disturbances from their interaction with the mean flow; it

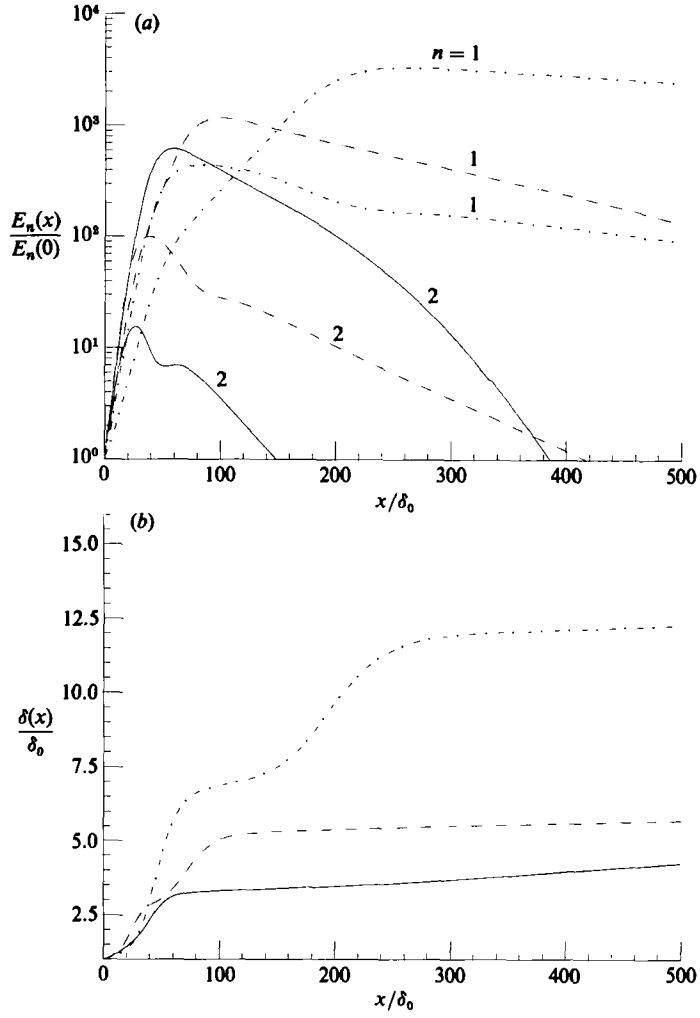


FIGURE 8. Effect of initial frequency parameter: (*a*) development of modal energy content and (*b*) mean-flow growth: ($\beta_0 = 0.075$(–·–·–), 0.18 (– – – –), 0.3 (——); $E_{10} = 0.12 \times 10^{-4}$, $E_{20} = 0.68 \times 10^{-4}$, $\theta = 0°$, $Re_0 = 71$).

also controls the overall amount of energy that each individual disturbance will extract from the mean flow throughout its development. In the case of $\beta_0 = 0.30$ the disturbance characterized by $2\beta_0 = 0.6$ starts at an amplification rate lower than that of its subharmonic and past its maximum amplification rate, as can be seen from the mean-flow interaction integral in figure 3. Subsequently the wave characterized by $\beta_0 = 0.3$ dominates throughout the development of the flow, as shown in figure 8(*a*), and is actually the 'fundamental' disturbance. The wave characterized by $2\beta_0$ is its first harmonic and despite the fact that the two-wave interaction mechanism acts in its favour ($\theta = 0°$), its role in the development of the flow is negligible. This is also apparent from the development of the mean flow for this case shown in figure 8(*b*), where the single plateau is attributed to the saturation of $E_1$ only.

In general decrease of the initial frequency parameter will increase the downstream amplification 'history' of each wave. The peaks in $E_1$ and $E_2$ are higher and occur at a later stage as the initial frequency parameter is decreased because of the implied

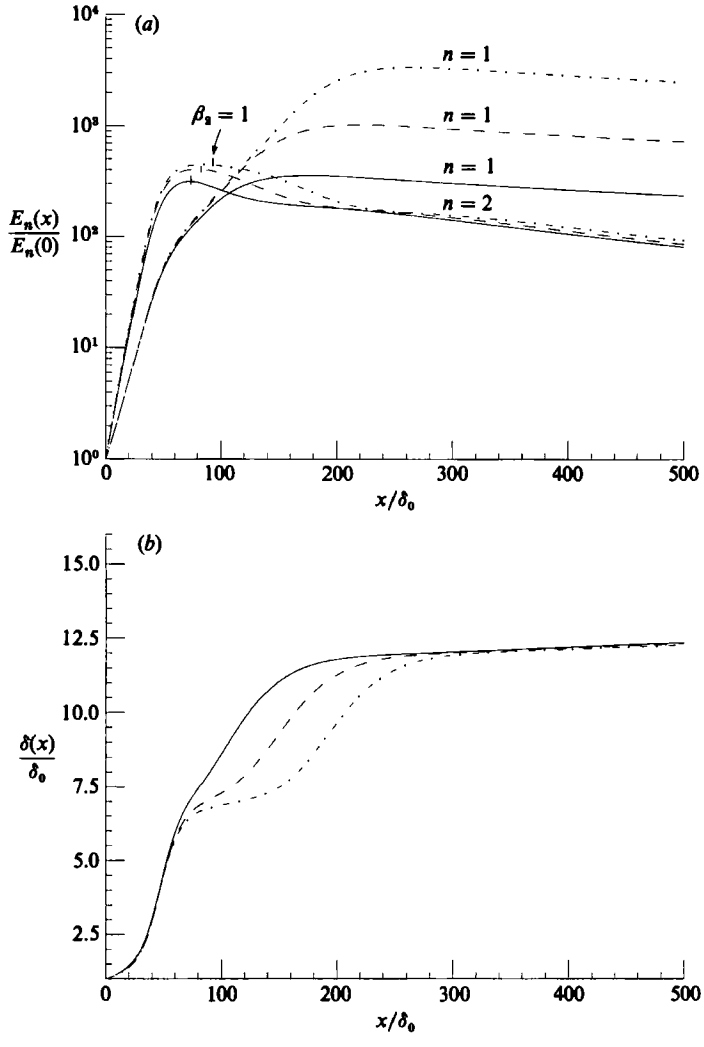


FIGURE 9(*a*, *b*). For caption see next page.

increase of the overall energy extracted from the mean. The growth of the mean flow is more pronounced for lower values of the initial frequency parameter owing to the same physical effect (figure 8*b*).

The discussion so far has been limited to the 'direct' effect of the initial frequency parameter on the development of the modal energy densities which is a consequence of the interaction with the mean flow. The effect of $\beta_0$ on the modal interaction mechanism is apparent from a comparison between the results presented in figures 6(*a*) and 7(*a*) for low and high $\beta_0$ respectively and for the case, say, where $\theta = 0°$. For high $\beta_0$, as pointed out earlier, the early interaction which is favourable to the subharmonic disturbance is practically absent unlike the case where the initial frequency parameter is low. This effect of $\beta_0$ on the modal interaction mechanism is, however, negligible compared to that of the phase angle. According to the above observations, we can conclude that the effect of the initial frequency parameter is essentially confined to influencing the interaction between the waves and the mean flow.

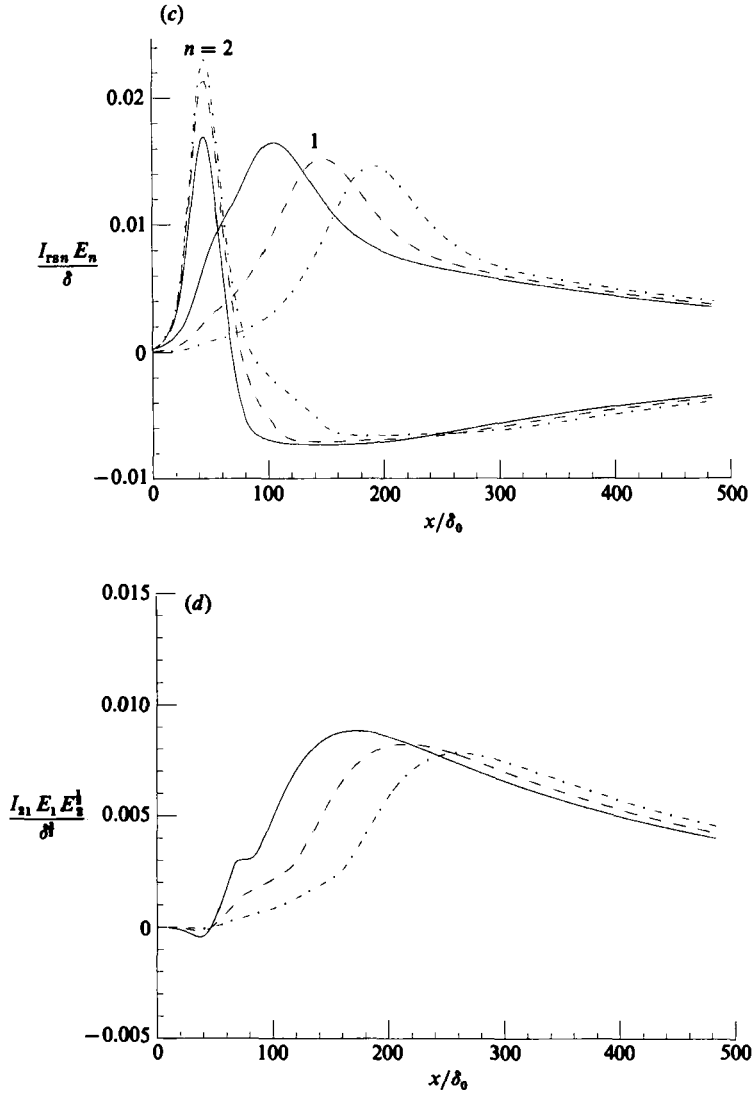


FIGURE 9. Effect of initial subharmonic energy density: (*a*) development of modal energy content, (*b*) mean-flow growth, (*c*) mode-production-term development and (*d*) development of binary-mode-interaction mechanism. ($E_{10} = 1.2 \times 10^{-4}$ (——), $0.4 \times 10^{-4}$ (– – – –), $0.12 \times 10^{-4}$ (–·–·–); $E_{20} = 0.68 \times 10^{-4}$, $\beta_0 = 0.075$, $\theta = 0°$, $Re_0 = 71$.)

### 4.3. *Effect of the initial energy density of the subharmonic*

The results of our calculations for three different initial energy densities of the subharmonic are given in figure 9(*a–d*) with all other initial parameters being fixed and a phase angle $\theta = 0°$. The peaks in $E_1/E_{10}$ are inversely proportional to $E_{10}$; therefore, the subharmonic reaches approximately the same peak level irrespectively of its initial energy density. The interaction of the subharmonic with the mean becomes maximum earlier with increasing $E_{10}$ as can be seen from figure 9(*c*), where we show the development of the wave-mean-interaction term. This accounts for the earlier peaking of $E_1$ and the subsequent earlier second plateau of the mean-flow

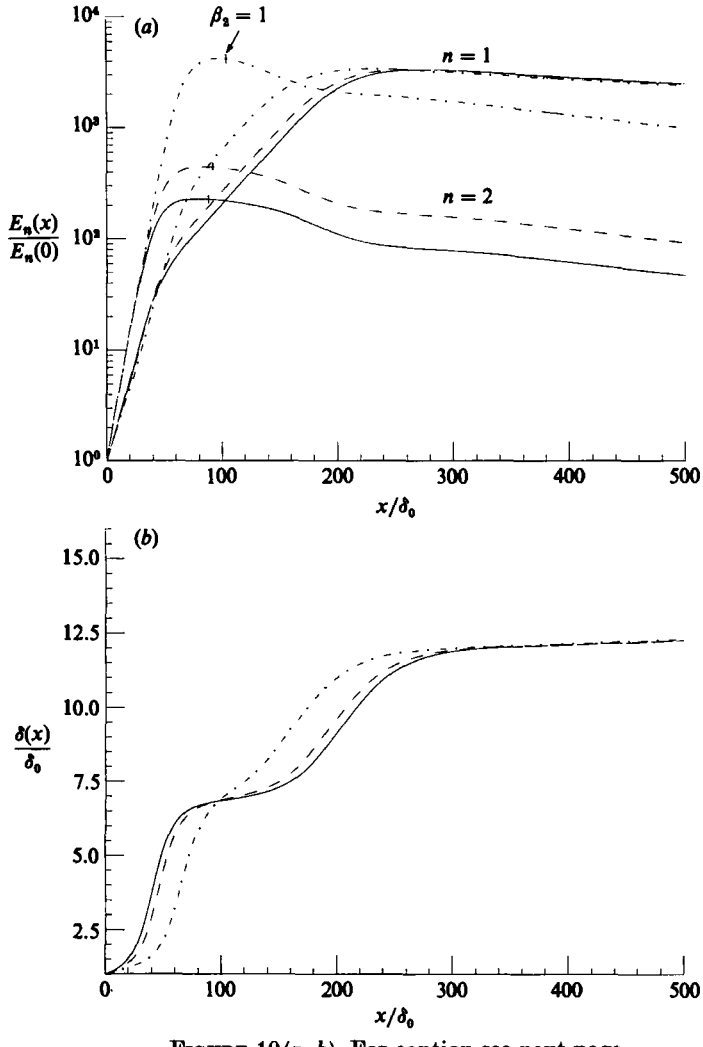


FIGURE 10(*a*, *b*). For caption see next page.

development shown in figure 9(*b*). The level of this plateau is independent of the initial energy density of the subharmonic as is the peak level of $E_1$. The two-wave interaction term, presented in figure 9(*d*), becomes strong earlier with increasing $E_{10}$. For this case of $\theta = 0°$ the two-wave interaction in the early stages of the modal development is in favour of the subharmonic, as discussed in an earlier section. These two observations explain the weakening of the interaction of the fundamental with the mean and the lower peak of $E_2$ with increasing $E_{10}$. This is also in agreement with Kelly's mechanism and results in a less prominent first plateau in the growth of the mean as we increase the initial subharmonic density. The location of $\beta_2 = 1$ (when $I_{rs2} = 0$) are indicated on figure 9(*a*) (and figure 10*a*) to give a better feeling for the nonlinear effects.

### 4.4. *Effect of the initial energy density of the fundamental*

The results of our calculations for three different initial energy densities of the fundamental are shown in figure 10(*a–d*). The peak value of the fundamental energy

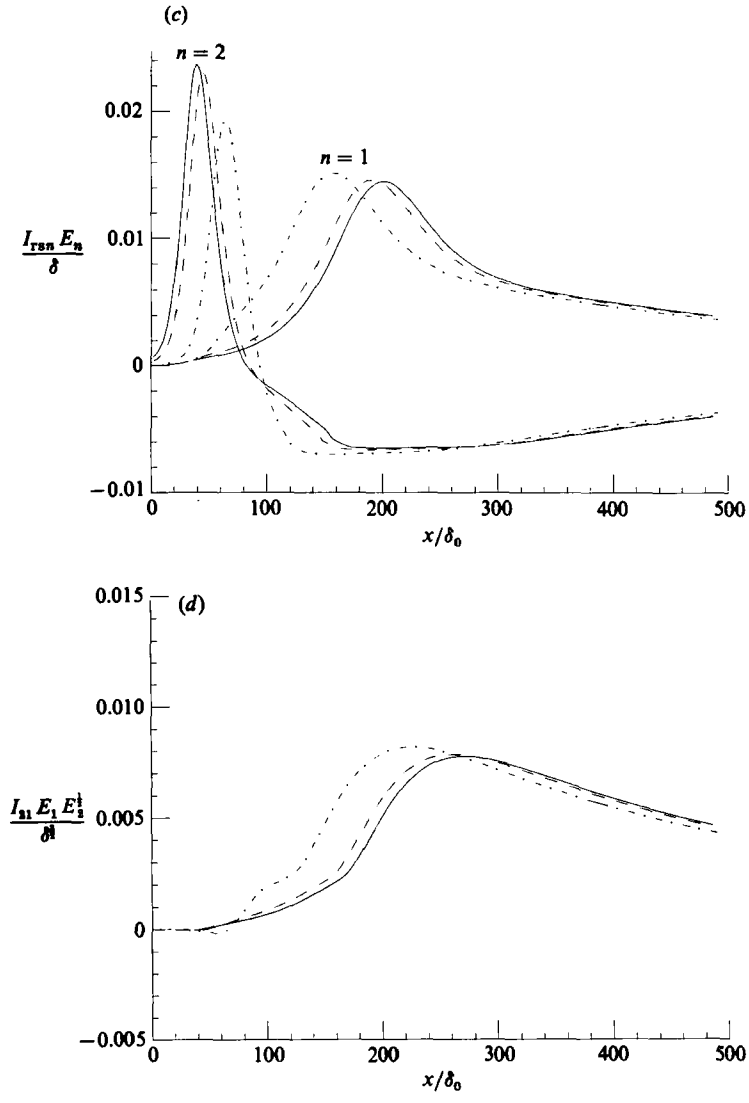


FIGURE 10. Effect of initial fundamental energy density: (*a*) development of modal energy content, (*b*) mean-flow growth, (*c*) mode-production-term development and (*d*) development of binary-mode-interaction mechanism. ($E_{20} = 13.6 \times 10^{-5}$ (——), $6.8 \times 10^{-5}$ (– – –), 0.6 (–·–·–) $\times 10^{-5}$; $E_{10} = 0.12 \times 10^{-4}$, $\beta_0 = 0.075$, $\theta = 0°$; $Re_0 = 71$.)

level $E_2$ is shown to be independent of its initial energy density since $E_2/E_{20}$ is inversely proportional to $E_{20}$ in figure 10(*a*). The peak value of the subharmonic also remains unaffected. Therefore the plateau levels in the growth of the mean presented in figure 10(*b*) are independent of $E_{20}$. The increase of the initial energy density of the fundamental intensifies the interaction with the mean (figure 10*c*) in its amplification region and therefore causes a faster growth of the shear layer as shown in figure 10(*b*). The interaction term between the subharmonic and the mean flow and the two-mode interaction term are inversely proportional to $\delta$ and $\delta^{\frac{3}{2}}$ (see (3.5) and (3.6)). Therefore, the faster growth of the mean accounts for the shift in the peaks of these two terms downstream (figure 10*c*, *d*), the subsequent weakening of the subharmonic and faster growth of the mean after the first plateau.

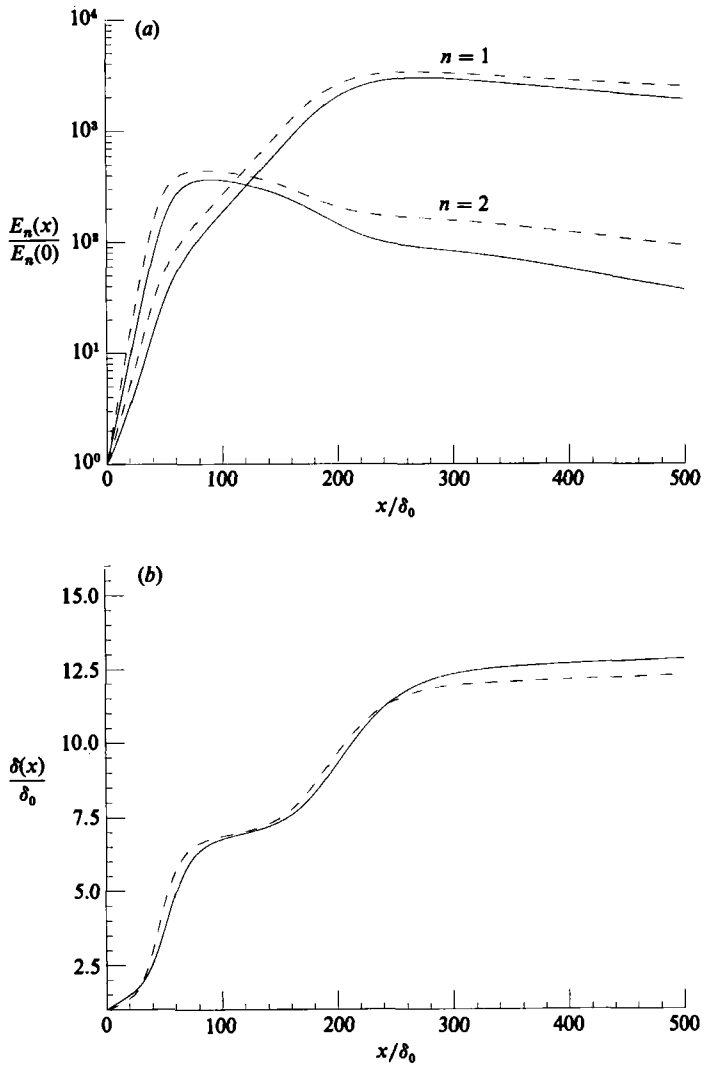


FIGURE 11. Effect of initial Reynolds number: (*a*) development of modal energy content and (*b*) mean-flow growth. ($Re$ = 71 (– – – –), 35.5 (——); $E_{10} = 0.12 \times 10^{-4}$, $E_{20} = 0.68 \times 10^{-4}$, $\beta_0 = 0.075$, $\theta = 0°$.)

### 4.5. *Effect of the initial Reynolds number*

The development of the energy levels of the fundamental and subharmonic disturbances, scaled by the corresponding initial values, are given in figure 11 (*a*) for $Re_0$ = 35.5 and 71. It can be seen that viscous dissipation has a very weak effect on the development of the modes. The fundamental and subharmonic peaks occur earlier and at a higher level with increasing $Re_0$. This of course was expected since viscous effects are weaker with increasing Reynolds number. The development of the mean flow is shown in figure 11 (*b*). The growth of the mean flow is faster for high $Re_0$ in the initial stages before the first plateau and is related to the growth of the fundamental. One would expect a slower growth of the mean when the Reynolds number is high, because of the viscous term $((1/Re_0)\, I_d/\delta)$ in (3.4). However, this term is negligible compared to the wave-production terms; thus the development of the mean is controlled primarily by the interaction with the two disturbances. We should

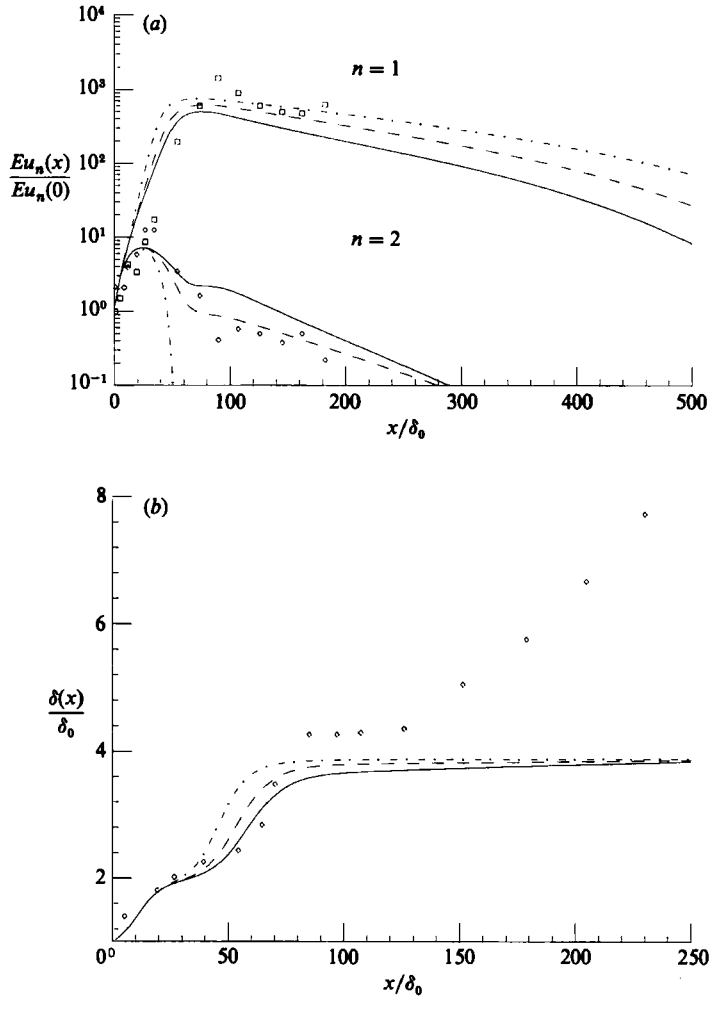


FIGURE 12. Comparison with Ho & Huang (1982) experiment (□, ◇): (*a*) development of modal energy content and (*b*) mean-flow growth. ($\theta = 0°$ (——), 80° (– – – –) and 180° (–·–·–); $Eu_{10} = 0.16 \times 10^{-4}$, $Eu_{20} = 0.48 \times 10^{-3}$, $\beta_0 = 0.26$, $Re_0 = 81$.)

point out that the use of the inviscid local solutions for the disturbances renders the interaction integrals independent of the Reynolds number; hence viscous effects have not been accounted for in full.

### 4.6. *Comparisons with experimental results of Ho & Huang (1982)*

The results of our calculation presented in this section are based on the experimental conditions corresponding to the measurements performed by Ho & Huang (1982). The initial subharmonic frequency parameter is taken to be $\beta_0 = 0.26$, giving a fundamental $2\beta_0 = 0.52$ which is very nearly at the maximum amplification rate according to the linear theory. These values were based on the initial maximum slope thickness $\delta_0$ at a location 1.43 cm downstream of the splitter plate, where the initial wake-type profile has developed into a hyperbolic tangent shear-layer profile, as reported by Ho & Huang (1982). The origin in the calculation, $x = 0$, is taken to be at the experimental 1.43 cm location. The relative phase between the fundamental and the subharmonic is left arbitrary (and therefore unknown) in the experiment.

We carried out the calculations for three different phase angles, namely $\theta = 0°$, $80°$ and $180°$.

The streamwise development of the energy levels of the streamwise component of the fundamental ($Eu_2$) and subharmonic ($Eu_1$) is qualitatively in very good agreement with the experiment as one can see from figure 12(*a*), particularly for the $\theta = 80°$ case. The location of the peaks in $Eu_1$ and $Eu_2$ are well in agreement with the experiment although the peak values themselves are underestimated. The growth of the shear layer shown in figure 12(*b*) also compares well with the experiments (Ho & Huang 1982) both qualitatively and quantitatively, in the region where the two wave modes are developing. The plateaux (attributed to the energy flow from the mean to the disturbances according to our previous discussion) as well as the approximate doubling of the thickness are evident in both the experiment and our results. In Ho & Huang's (1982) experiments, the shear layer continues to spread after the plateau regions (figure 12*b*); it is most likely that transition has taken place in that the existing fine-grained turbulence having been sufficiently strained by the coherent structures is now contributing towards the mean-flow spreading rate via the fine-grained turbulence Reynolds-stress mechanism (Liu 1981). This mechanism is not present in our formulation since we have not taken into account the fine-grained turbulence. Therefore this latter spread of the mean flow cannot be predicted by our calculations.

Apart from the fine-grained turbulence, there are many other less dominant disturbance-wave modes present in the experiments of Ho & Huang (1982) to which the shear layer is sensitive. This fact together with the arbitrariness of the phase angle in the experiment leads to the conclusion that the quantitative details of the shear layer are not expected to be described by the idealized two-mode problem in the absence of weak fine-grained turbulence and other (not necessarily weak) modes. However, the problem solved here brings out the dominant physical mechanisms in the growth and decay of the overlapping fundamental and subharmonic disturbances, as well as the important effect of the initial conditions and relative phase angle.

### 4.7. *Further discussion of observations*

Experiments, of a preliminary nature, were performed by Zhang *et al.* (1985) in which both the fundamental and subharmonic disturbances in a mixing layer were forced at different relative phases. An interpretation of their results on the relative amplification rates is given here. (The issue of the relative importance of the wake effect on disturbance development in the mixing region remains open (Zhang *et al.* 1985; Miau & Karlsson, 1986).) Zhang *et al.* (1985) found that the fundamental-component amplification rates remain unaffected by the relative phase angles but not those of the subharmonic (see figure 7, Zhang *et al.* 1985).

We can recast the energy equations (3.5) and (3.6) into the form for the 'amplification rates' using $\mathrm{d}\ln En/\mathrm{d}x$, where $n = 1$ (subharmonic) and 2 (fundamental). The 'amplification rates' obtained from the right-hand sides of (3.5) and (3.6) are of the form

$$\frac{\mathrm{d}\ln E_1}{\mathrm{d}x} \sim \left(\frac{1}{\delta} I_{\mathrm{rs1}} - \frac{I_{\mathrm{d1}}}{Re_0 \delta^2}\right) - \frac{I_{21} E_2}{\delta^{\frac{3}{2}}},$$

$$\frac{\mathrm{d}\ln E_2}{\mathrm{d}x} \sim \left(\frac{1}{\delta} I_{\mathrm{rs2}} - \frac{I_{\mathrm{d2}}}{Re_0 \delta^2}\right) + \frac{I_{21} E_2^{\frac{1}{2}}}{\delta^{\frac{3}{2}}} \left(\frac{E_1}{E_2}\right).$$

The first term on the right is the net 'production' rate from the mean flow and the second term is the mode-energy-transfer term. The mode-interaction integral $I_{21}$ is dependent upon the relative phase between the modes (see figure 4) and is actually

a nonlinear effect for which the simple 'universal' interpretation via the linear theory (Zhang *et al.* 1985) would not suffice as is evidenced from the disturbance-amplitude dependence. In Zhang *et al.*'s (1985) experiments, the fundamental amplitude is about an order of magnitude larger than that of the subharmonic, thus the factor $E_1/E_2 \ll 1$ renders the 'amplification rate' for $E_2$ dependent on the net production from the mean flow only and more or less independent of the energy transfer to the subharmonic (and thus independent of the relative phase). On the other hand, in the 'amplification-rate' relation for the subharmonic ($E_1$), the factor ($E_1/E_2$) does not occur. If $E_2^{\frac{1}{2}}$ is sufficiently large so as to render $I_{21}E_2^{\frac{1}{2}}/\delta^{\frac{3}{2}}$ comparable to the net mean-flow production, then the 'amplification rate' of $E_1$ would depend on the relative phase relation. The correction to the amplification rate due to the net mean-flow production depends on the sign of $I_{21}$. In the initial developing region when the scaled frequency parameter $\beta_1 \approx 0.22$ (the subharmonic value for the present $R = 0.31$), the sign of $I_{21}$ is consistent with that indicated by Zhang *et al.*'s (1985) interpretation (their figure 7). It is clear that the phase relation is not the only parameter in this problem. The initial and local shear-layer-thickness development as well as the initial and local mode amplitudes all contribute to the nonlinear problem.

This work was partially supported by the National Aeronautics and Space Administration, Langley Research Center through Grant NAG1-379, Lewis Research Center through Grant NAG3-673; The National Science Foundation, Fluid Mechanics and Hydraulics Program through Grant MSM83-20307 and The Applied and Computational Mathematics Program, Defense Advanced Research Projects Agency through its University Research Initiative Program. Partial support of travel funds from NATO Research Grant 343/85 and NSF Grant INT85-14196 are also acknowledged.

## Appendix. Two-mode interaction integrals

$$I_{\mathrm{m}} = -\frac{1}{2}\left[\int_{-\infty}^{0}(1-R\tanh\eta)\,[(1-R\tanh\eta)^2-(1+R)^2]\,\mathrm{d}\eta + \int_{0}^{\infty}(1-R\tanh\eta)\,[(1-R\tanh\eta)^2-(1-R)^2]\,\mathrm{d}\eta\right] = 2R^2(\tfrac{3}{2}-\ln 2),$$

$$I_1(\delta) = 1-R\int_{-\infty}^{+\infty}\tanh\eta\{|\phi_1'|^2+|\alpha_1\phi_1|^2\}\,\mathrm{d}\eta,$$

$$I_2(\delta) = 1-R\int_{-\infty}^{+\infty}\tanh\eta\{|\phi_2'|^2+|\alpha_2\phi_2|^2\}\,\mathrm{d}\eta,$$

$$I_{\mathrm{rs1}} = 2R\int_{-\infty}^{+\infty}\mathrm{sech}^2\eta\ \mathrm{Im}\,(\alpha_1\phi_1\bar{\phi}_1')\,\mathrm{d}\eta,$$

$$I_{\mathrm{rs2}} = 2R\int_{-\infty}^{+\infty}\mathrm{sech}^2\eta\ \mathrm{Im}\,(\alpha_2\phi_2\bar{\phi}_2')\,\mathrm{d}\eta,$$

$$I_{21} = 2\int_{-\infty}^{+\infty}\mathrm{Im}\{\mathrm{e}^{i\theta}\{\bar{\alpha}_2[\bar{\phi}_2'(\phi_1'^2+\alpha_1^2\phi_1)+\alpha_1\bar{\alpha}_2\bar{\phi}_2\phi_1\phi_1']+\alpha_1\phi_1\phi_1'\bar{\phi}_2''\}\}\,\mathrm{d}\eta,$$

$$I_{\mathrm{d}} = \int_{-\infty}^{+\infty} R^2 \operatorname{sech}^4 \eta \, \mathrm{d}\eta = \frac{4R^2}{3},$$

$$I_{\mathrm{d1}} = 2|\alpha_1|^2 + 2\int_{-\infty}^{+\infty} \{|\phi_1''|^2 + |\alpha_1 \phi_1'|^2\} \, \mathrm{d}\eta,$$

$$I_{\mathrm{d2}} = 2|\alpha_2|^2 + 2\int_{-\infty}^{+\infty} \{|\phi_2''|^2 + |\alpha_2 \phi_2'|^2\} \, \mathrm{d}\eta,$$

where Im denotes the imaginary part and $\overline{\phi}$ denotes the complex conjugate of $\phi$.

## REFERENCES


ALPER, A. & LIU, J. T. C. 1978 On the interactions between large-scale structure and fine grained turbulence in a free shear flow. II. The development of spatial interactions in the mean. *Proc. R. Soc. Lond.* A **395**, 497–523.

BROWAND, F. K. 1966 An experimental investigation of the instability of an incompressible separated shear layer. *J. Fluid Mech.* **26**, 281–307.

FIEDLER, H. E., DZIOMBA, B., MENSING, P. & RÖSGEN, T. 1981 Initiation, evolution and global consequences of coherent structures in turbulent shear flows. In *The Role of Coherent Structures in Modelling Turbulence and Mixing* (ed. J. Jimenez). Lecture Notes in Physics, vol. 136, pp. 219–251. Springer.

FREYMUTH, P. 1966 On transition in a separated laminar boundary layer. *J. Fluid Mech.* **25**, 683–704.

GASTER, M., KIT, E. & WYGNANSKI, I., 1985 Large-scale structures in a forced turbulent mixing layer. *J. Fluid Mech.* **150**, 23–39.

HO, C. M. & HUANG, L. S. 1982 Subharmonics and vortex merging in mixing layers. *J. Fluid Mech.* **119**, 443–473.

KELLY, R. E. 1967 On the stability of an inviscid shear layer which is periodic in space and time. *J. Fluid Mech.* **27**, 657–689.

LIN, C. C. 1955 *The Theory of Hydrodynamic Stability*. Cambridge University Press.

LIU, J. T. C. 1981 Interaction between large-scale coherent structures and fine-grained turbulence in free shear flows. In *Transition and Turbulence* (ed. R. E. Meyer), pp. 167–214. Academic.

LIU, J. T. C. 1987 Contributions to the understanding of large-scale coherent structures in developing free turbulent flows. *Adv. Appl. Mech.* **26** (in press).

LIU, J. T. C. & LEES, L. 1970 Finite amplitude instability of the compressible laminar wake. Strongly amplified disturbances. *Phys. Fluids* **13**, 2932–2938.

LIU, J. T. C. & MERKINE, L. 1976 On the interactions between large-scale structure and fine-grained turbulence in a free shear flow. I. The development of temporal interactions in the mean. *Proc. R. Soc. Lond.* A **352**, 213–247.

LIU, J. T. C. & NIKITOPOULOS, D. E. 1982 Mode interactions in developing shear flows. *Bull. Am. Phys. Soc.* **27**, 1192.

MACK, L. M. 1965 Computation of the stability of the laminar compressible boundary layer. *Meth. Comp. Phys.* **4**, 274–299.

MANKBADI, R. R. 1985 On the interaction between fundamental and subharmonic instability waves in a turbulent round jet. *J. Fluid Mech.* **160**, 385–419.

MIAU, J.-J. & KARLSSON, S. K. F. 1986 Evolution of flow in the developing region of the mixing layer with a laminar wake as initial condition. *Phys. Fluids* **29**, 3598–3607.

MIKSAD, R. W. 1972 Experiments on the nonlinear stages of free shear layer transition. *J. Fluid Mech.* **56**, 695–719.

MIKSAD, R. W. 1973 Experiments on nonlinear interactions in the transition of a free shear layer. *J. Fluid Mech.* **59**, 1–21.

NIKITOPOULOS, D. E. 1982 Nonlinear interaction between two instability waves in a developing shear layer. ScM thesis. Brown University, Providence, R.I.

RUE-SU KO, D. R. S., KUBOTA, T. & LEES, L. 1970 Finite disturbance effect on the stability of a laminar incompressible wake behind a flat plate. *J. Fluid Mech.* **40**, 315–341.

SATO, H. 1959 Further investigation on the transition of two-dimensional separated layer at subsonic speeds. *J. Phy. Soc. Japan* **14**, 1797–1810.

STUART, J. T. 1958 On the nonlinear mechanics of hydrodynamic stability. *J. Fluid Mech.* **4**, 1–21.

STUART, J. T. 1962 Nonlinear effects in hydrodynamic stability. In *Proc. 10th Int. Congr. Appl. Mech.* (ed. F. Rolla & W. T. Koiter), pp. 63–97. Elsevier.

WILLE, R. 1963 Beiträge zur Phänomenologie der Freistrahlen. *Z. Flugwiss.* **11**, 222–233.

WILLIAMS, D. R. & HAMA, F. R. 1980 Streaklines in a shear layer perturbed by two waves. *Phys. Fluids* **23**, 442–447.

WINANT, C. D. & BROWAND, F. K. 1974 Vortex pairing, the mechanism of turbulent mixing-layer growth at moderate Reynolds number. *J. Fluid Mech.* **63**, 237–255.

WYGNANSKI, I. & FIEDLER, H. E. 1970 The two-dimensional mixing region. *J. Fluid Mech.* **41**, 327–361.

WYGNANSKI, I., OSTER, D., FIEDLER, H. & DZIOMBA, B. 1979 On the perserverance of a quasi-two-dimensional eddy-structure in a turbulent mixing layer. *J. Fluid Mech.* **93**, 325–335.

ZAAT, J. A. 1958 In *Boundary Layer Research* (ed. H. Görtler), p. 127. Springer.

ZHANG, Y. Q., HO, C. M. & MONKEWITZ, P. 1985 The mixing layer forced by fundamental and subharmonic. In *Laminar–Turbulent Transition, IUTAM Symp., Novosibirsk 1984* (ed. V. V. Kozlov), pp. 385–395. Springer.